
^{99m}Tc -MIBI Scintimammography Using a Dedicated Nuclear Mammograph

Carlo L. Maini, Francesco de Notaristefani, Anna Tofani, Francesca Iacopi, Rosa Sciuto, Alessandro Semprebene, Tiziana Malatesta, Franco Vittori, Fabrizio Frezza, Claudio Botti, Salvatore Giunta and Pier Giorgio Natali

Departments of Nuclear Medicine, Medical Physics, First Oncologic Surgery, Diagnostic Radiology and Immunology, Regina Elena Cancer Institute, Rome; and National Institute of Nuclear Physics (INFN), Section of Rome 1 at Universities of Roma-Tre and La Sapienza, Rome, Italy

This study reports on a prototype single-photon emission mammograph (SPEM) dedicated to ^{99m}Tc -hexakis-2-methoxyisobutyl isonitrile (MIBI) scintimammography. Main technical features are reported together with physical performance. Preliminary patient data are also reported. **Methods:** The SPEM detector head is composed of a CsI(Tl) scintillating array coupled to a Hamamatsu R3292 position-sensitive photomultiplier tube with crossed-wire anode. The high-resolution collimator is 35-mm thick with a 1.7-mm hole diameter and a 0.2-mm septal thickness. The electronic acquisition system is composed of five integrated cards with computation based on high-speed programmable microprocessors. The readout electronics include correction maps for on-line energy correction and spatial uniformity. The small size of the detector head allows the use of mechanical breast compression to minimize detection distance and tissue scatter. After physical SPEM performance evaluation in vivo scintimammography was performed in 29 patients and was compared with a state-of-the-art Anger camera. **Results:** The SPEM showed an intrinsic spatial resolution of 2 mm, an energy resolution of 23% FWHM at 122 keV and spatial uniformities of 18% (integral) and 13.5% (differential). The SPEM imaged one 0.4-cm carcinoma missed by the Anger camera and resolved as separate lumps an irregular focal uptake on the Anger camera image. The remaining cases yielded concordant results. **Conclusion:** The SPEM prototype presented in this study shows adequate physical characteristics for ^{99m}Tc -MIBI scintimammography.

Key Words: ^{99m}Tc -hexakis-2-methoxyisobutyl isonitrile; scintimammography; imaging device

J Nucl Med 1999; 40:46–51

Technetium- 99m -hexakis-2-methoxyisobutyl isonitrile (MIBI) scintimammography is a promising new imaging tool for the diagnosis of breast carcinoma (1–7) and for the assessment of its response to chemotherapy (8). Reported sensitivities and specificities for breast cancer diagnosis range from 84% to 94% for the former and from 72% to 94% for the latter (9,10) and are clearly affected by referral

biases. False-positives are commonly observed in benign lesions characterized by enhanced metabolism, such as some fibroadenomas (1–7), and false-negatives may be due to several factors, including low metabolic rate of some tumors and overexpression of multidrug resistance glycoproteins, such as Pgp-170 (11–13) and/or MRP-190 (14), which affect MIBI efflux from the cancer cell.

Sensitivity is also dependent on the physical features of the detecting system, with lesion size being a key factor affecting detectability (9,10). Anger cameras are limited by a relatively poor intrinsic spatial resolution and the detection geometry is suboptimal because of the distance between the breast and the detector. Very high intrinsic spatial resolution values (≤ 2 mm) can be achieved by coupling an array of scintillating crystals to a position-sensitive photomultiplier tube (PSPMT) (15–17). The technique has been exploited for the development of a compact single-photon emission mammograph (SPEM; manufactured with the support of Preciosa Crytur, Turnov, Czech Republic) prototype that offers the additional advantage of a minimal distance between the breast and the detector. This article describes the SPEM prototype and reports the preliminary data on clinical performance.

MATERIALS AND METHODS

Patients and Study Design

The study was designed as pilot phase I trial. Informed consent and ethical committee approval was obtained.

Twenty-nine consecutive women referred for conventional Anger camera scintimammography as part of their routine diagnostic work-up entered the study. The inclusion criteria was a breast lesion under 2 cm at clinical examination, at conventional imaging (mammography or sonography), or at both. The median age was 50 y with a range of 21–79 y. The patients selected for the study underwent imaging with the SPEM prototype immediately after Anger camera scintimammography, thus requiring no additional ^{99m}Tc -MIBI administration. In all patients, Anger camera scintimammography was performed 15 min after radiotracer administration. The two sets of scintigrams were obtained and were blindly interpreted by two well-trained nuclear medicine physicians.

In each patient, an indwelling catheter was placed in the arm on the contralateral side of the breast lesion and 740 MBq (20 mCi)

Received Jan. 6, 1998; revision accepted May 13, 1998.

For correspondence or reprints contact: Carlo L. Maini, MD, PhD, La Pietra Pizzuta, 03010 Patrica—FR—Italy.

^{99m}Tc -MIBI (Cardiolite; DuPont Pharma, Billerica, MA) were administered and were followed by a saline solution flush to clear the vessels. The labeling and quality control procedures were performed according to the manufacturer's instructions.

All patients underwent surgery after the nuclear studies, and a pathological diagnosis was obtained according to World Health Organization (WHO) criteria.

SPEM Prototype

The SPEM prototype is shown in Figure 1A. The detector head is composed of a CsI(Tl) scintillating array 0.3-cm thick manufactured by Hilger Analytical (Margate, United Kingdom), covering a total of 10×10 cm field of view (FOV), coupled to a 5-in. (12.7-cm) diameter Hamamatsu R3292 PSPMT with crossed-wire anode. The Hamamatsu R3292 has 28X + 28Y anode wires ending on four terminations (X_A , X_B , Y_C , Y_D). For each scintillation event, these four signals are summed to achieve the total energy information, while position computation is performed by the "resistive chain" algorithm (18). The Hamamatsu R3292 has a quantum efficiency of its alkali photocathode around 23% (Hamamatsu Photonics TSU PSPMT data sheet, Shizouka, Japan, 1995). The single-crystal pillars have a 2×2 mm cross section and are optically isolated by an epoxy diffusive layer 300- μm thick. The high-resolution collimator, 35-mm thick with a 1.7-mm hole diameter and a 0.2-mm septal thickness, is manufactured by Von Gahlen (Didam, The Netherlands). The collimator was designed with a spatial resolution of 7.5 mm at 10 cm distance from its surface and a sensitivity of 300 counts/min/ μCi . The whole head is shielded by a 2-cm-thick lead box and is mounted on a rotating arm that allows a full rotation around two orthogonal axes. The rotating arm is equipped with a compressing device designed to keep the

breast in place and to reduce the distance and the scattering medium between the lesion and the detector.

The electronic acquisition system, developed by Crytur-Tescan (Brno, Czech Republic), is described in Figure 1B. It is composed of five integrated cards with computation based on programmable microprocessors dedicated to high-speed processing (ADSP 2171; Analog Devices, Norwood, MA). Processed data are sent to a personal computer with a dedicated interface through a serial optical cable with a maximum transfer rate of 5 Mbits per second. The readout electronics have a dedicated memory space in which correction maps are loaded for on-line energy correction during acquisition to improve energy resolution.

Physical characterization of the SPEM mammograph included measures of intrinsic spatial resolution, spatial linearity, global energy resolution, spatial integral and differential uniformity, point sensitivity and counting rate linearity. National Electronics Manufacturers Association (NEMA) norms were followed when applicable.

Anger Camera Scintimammography

Conventional scintimammography was performed with a state-of-the-art Anger gamma camera (Prism 2000; Picker Medical Systems, Cleveland, OH) equipped with a high-resolution, parallel-hole collimator yielding a spatial resolution of the system of 9.5 mm FWHM at 10 cm. Digital planar images (256×256 matrix size, 1.5 zoom, with a minimum 1000 kcounts) were acquired with the patient in the supine position (anterior and oblique views) and in the prone position (lateral views) using a dedicated foam rubber mattress. Acquisition was prolonged to 10 min in case of negative scans. Scintigraphy was defined as positive on the basis of focal tracer uptake in the breast lesion under evaluation.

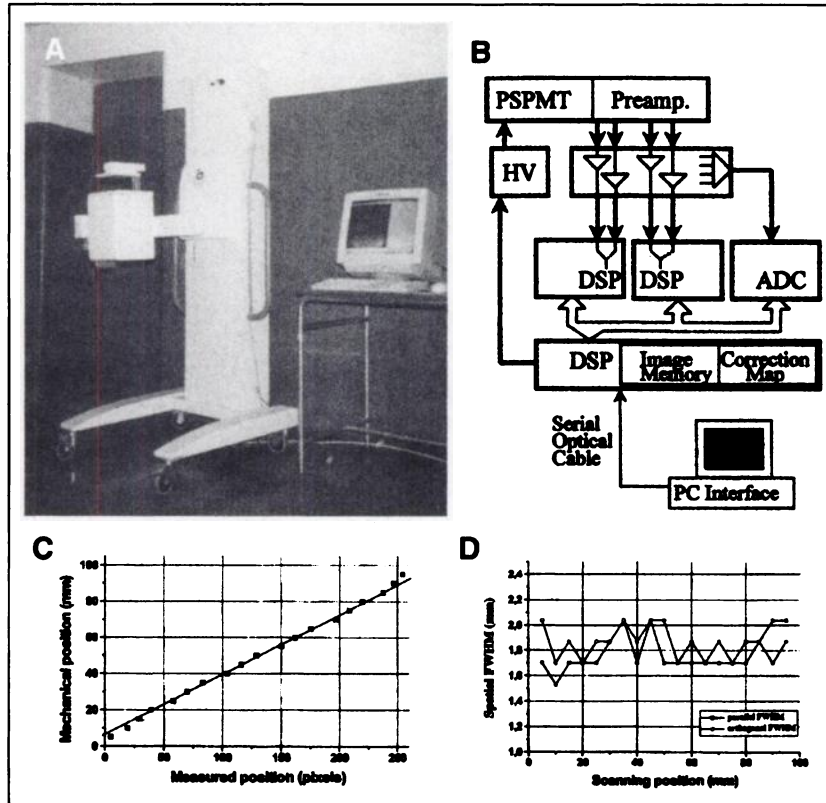


FIGURE 1. (A) SPEM prototype. Compressor is evident on top of detection head. (B) Block diagram of electronic acquisition system. PSPMT = position-sensitive photomultiplier tube; HV = high-voltage supply; DSP = digital signal processing cards; ADC = analog digital converter. (C) Spatial linearity plot: 5-mm scanning step with 1-mm collimated ^{57}Co source. (D) Parallel and orthogonal FWHM spatial resolution: 5-mm scanning step with 1-mm collimated ^{57}Co source.

SPEM Scintimammography

SPEM scintigraphy was performed immediately after the Anger camera acquisition. Patients sat with their hands placed behind their own head; the selected breast was mildly compressed between the square-shaped detector and the camera's breast compressor. Craniocaudal, mediolateral and oblique projections were obtained with a matrix size of 64×64 . In selected cases, an anterior projection with no breast compression was also acquired. A preset count acquisition of 200 kcount/image was used leading to ~15-min acquisition time for each projection. SPEM scintigraphy was defined as positive on the basis of focal tracer uptake in the breast lesion under evaluation.

RESULTS

Physical Measures

Intrinsic spatial resolution and spatial linearity can be evaluated by the data generated by a 5-mm pitch scan performed on x- and y-axes with a 1-mm collimated ^{57}Co source with the support of an optical bench (Figs. 1C and D). The detector maintains a good linear behavior on almost all its surface. The position linearity plot shows a slight "step behavior" due to the fact that the collimation diameter for the scanning is comparable to crystal cross section, but this effect is strongly reduced in operative conditions because the collimation hole diameter is 1.7 mm. Figure 1D shows the intrinsic FWHM spatial resolution reporting the value in millimeters for each step of the scanning along one of the orthogonal axes. The plot reports the measures relative to

both sections orthogonal and parallel to the axis. The average value of FWHM is about 1.8 mm, but because the sampling step is 2 mm (cross section of the crystal), the latter represents the true value of intrinsic spatial resolution of the detector.

Detector uniformity and global energy resolution were evaluated by a flood field irradiation with a point source of ^{57}Co . The flood field spectrum, after the application of the energy correction procedure, showed a 23% FWHM energy resolution (Fig. 2C). This value, although not optimal, can be considered a good result in relation to the quantity of rejectable scattered radiation (19). Raw spatial integral uniformity was 30% and reached 18% after the application of software count correction procedure (Figs. 2A and B), whereas the differential raw spatial uniformity was 21% and reached 13.5% after the same procedure.

Point sensitivity and counting rate linearity were evaluated for a range of activities of 0.37 MBq–1.85 GBq (0.1–50 mCi) with a $^{99\text{m}}\text{Tc}$ source in air and with 2 cm of tissue equivalent scattering media. A good linearity is evident up to 370 MBq (Fig. 2D), which is more than adequate for the activity ranges of scintimammography.

Clinical Results

Clinical, pathological and imaging data are reported in Table 1. Nineteen out of 29 patients had cancers. Prevalence of palpable lesions was 12 out of 19 cancers and 6 out of 10 benign lesions. Figure 3 shows two cases of true-positive

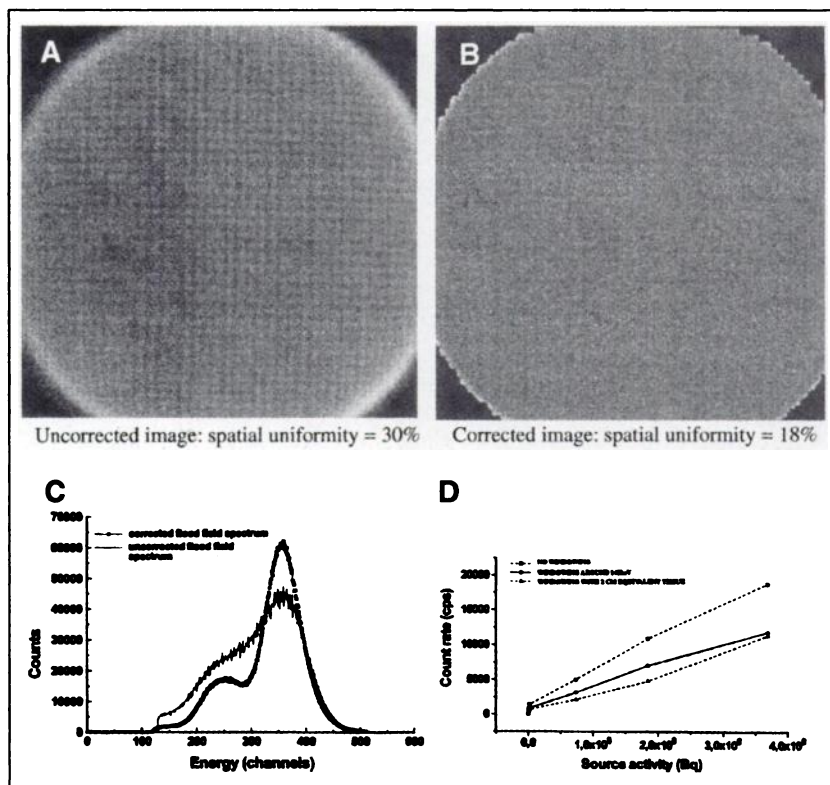


FIGURE 2. (A) Raw intrinsic spatial uniformity. (B) Intrinsic spatial uniformity after software correction. (C) Global energy resolution at 122 keV without and with on-line correction. (D) Counting rate linearity including no windowing (normal) and windowing (lower limit: 110 keV, upper limit: 170 keV) in air and with 2 cm of tissue equivalent scattering medium.

TABLE 1
Patient Data for Breast Cancers and Benign Breast Lesions

| Patient no. | Age (y) | Histology | Size (cm) | Physical examination | Anger* | SPEM* | Mammography | Sonography |
|------------------------------|---------|-----------|-----------|----------------------|--------|-------|-------------|------------|
| Breast cancers | | | | | | | | |
| 1 | 47 | DI | 0.4 | NP | - | + | S | S |
| 2 | 64 | DI | 0.7 | NP | + | + | S | S |
| 4 | 49 | DI | 1 | P | + | + | S | S |
| 5 | 67 | LI | 0.6 | NP | + | + | M | np |
| 8 | 34 | DI | 0.8 | P | - | - | np | S |
| 11 | 32 | DI | 1 | NP | - | - | M | np |
| 12 | 37 | DI | 1.2 | P | + | + | S | S |
| 15 | 55 | DI | 0.8 | NP | + | + | M | np |
| 16 | 38 | DI | 0.6 | NP | + | + | S | S |
| 17 | 58 | DI | 0.8 | NP | - | - | S | np |
| 18 | 48 | LI | 1.2 | P | + | + | M | np |
| 22 | 75 | DI | 1.5 | P | + | + | S | np |
| 23 | 21 | DI | 1.2 | P | + | + | np | S |
| 24 | 69 | LI | 1.3 | P | + | + | S | np |
| 25 | 74 | DI | 1.8 | P | + | + | M | np |
| 26 | 46 | DI | 1.57 | P | + | + | S | np |
| 27 | 58 | DI | 1.5 | P | + | + | S | np |
| 28 | 79 | LI | 1.08 | P | + | + | M | np |
| 29 | 77 | DI | 1.5 | P | + | + | M | np |
| Benign breast lesions | | | | | | | | |
| 3 | 47 | FA | 1.4 | P | + | + | S | S |
| 6 | 34 | FA | 1.7 | P | - | - | np | S |
| 7 | 40 | FA | 1 | NP | - | - | S | S |
| 9 | 53 | FA | 0.5 | NP | - | - | B | S |
| 10 | 50 | FA | 1.1 | P | + | + | S | S |
| 13 | 62 | LP | 1.3 | P | - | - | S | np |
| 14 | 62 | FA | 0.7 | NP | - | - | S | S |
| 19 | 45 | FA | 1.2 | P | - | - | S | np |
| 20 | 56 | FA | 0.5 | NP | - | - | S | S |
| 21 | 41 | FA | 1.3 | P | - | - | B | B |

*+ = evident focal MIBI uptake; - = no focal MIBI uptake.

SPEM = single-photon emission mammograph; MIBI = hexakis-2-methoxyisobutyle isonitrile.

DI = invasive ductal carcinoma; NP = nonpalpable lesion; S = suspicious; P = palpable lesion; LI = invasive lobular carcinoma; M = malignant; np = not performed; FA = fibroadenoma; B = benign; LP = lipoma.

scans with both imaging techniques. Sensitivities were 79% for the Anger camera and 84% for the SPEM, with the latter identifying all the cancers imaged by the former and one of 0.4 cm that was not imaged (patient 1 in Figs. 4A and C). Superior SPEM resolution resolved as three separate lesions the irregular focal uptake seen in patient 28 with the Anger camera (Figs. 4B and D). Three carcinomas showed no uptake with both imaging techniques. Specificity was 80% for both Anger camera and SPEM with two fibroadenomas showing focal ^{99m}Tc-MIBI uptake.

DISCUSSION

Radiological mammography remains the cornerstone of breast carcinoma imaging with sonography playing a useful secondary role. However, radiological mammography is now perceived as suboptimal in the dense breast and the

operated breast and in the assessment of the response to chemotherapy (6-10). Both MRI (20,21) and ^{99m}Tc-MIBI scintimammography have been proposed as second-line imaging procedures in selected cases. It is now well perceived that ^{99m}Tc-MIBI scintimammography can result in both false-positive scans, typically in metabolical hyperactive fibroadenomas (1-7), and false-negative scans, which can be due to metabolical cancer features such as overexpression of Pgp-170 (11-13) and/or MRP-190 (14) or to detection limitations of current Anger cameras. These limitations are due to limited resolution and to a clearly inadequate geometrical setup because of the constrained distance between the breast and the detector. The SPEM prototype described in this article addresses both.

Several dedicated nuclear mammograph prototypes have been developed (22,23) including a high-resolution YAP

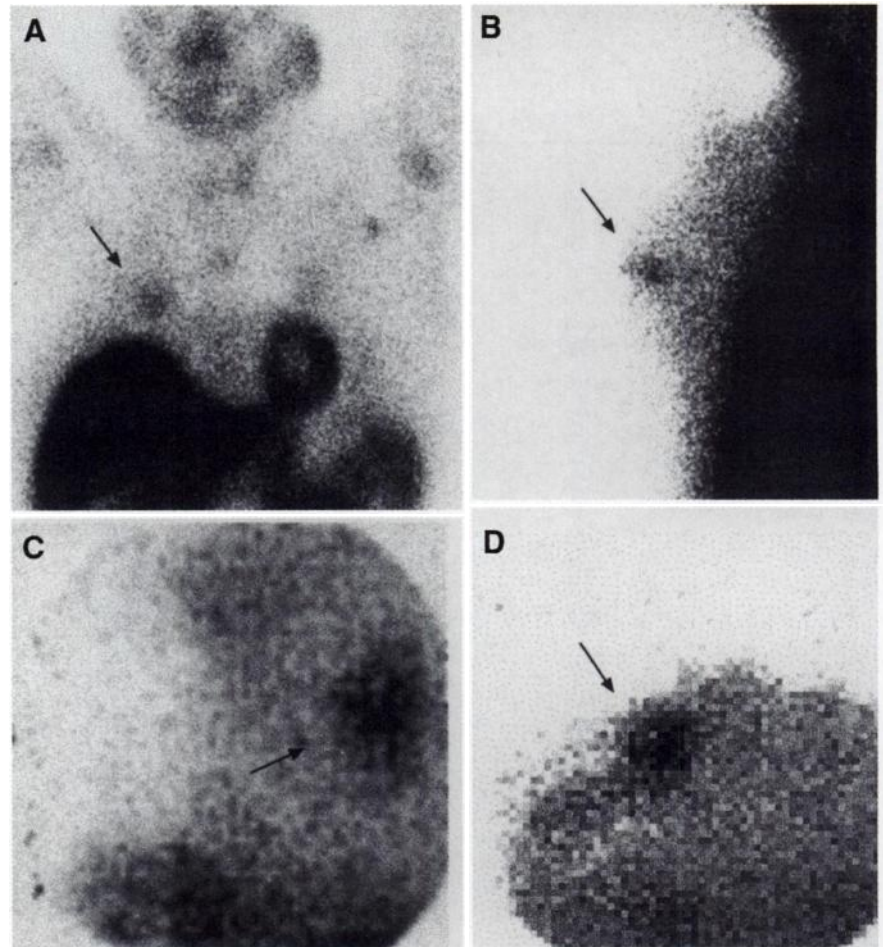


FIGURE 3. Two cases of true-positive ^{99m}Tc -MIBI uptake in ductal carcinomas. (A) Anger camera anterior view and (C) SPEM anterior view of right breast in patient 12. (B) Anger camera lateral view and (D) SPEM craniocaudal view of left breast in patient 4.

camera equipped with a Hamamatsu crossed-wire anode PSPMT (24,25) whose energy resolution is, however, unacceptably low for imaging in high-scatter geometries typical of clinical scintimammography. The SPEM prototype substitutes a CsI(Tl) crystal to the YAP:Ce. The physical properties of CsI(Tl) have been reported (26,27); CsI(Tl) detects photons around 140 keV with an efficiency superior to YAP:Ce, allowing the reduction of crystal thickness from 10 to 3 mm. The high output of CsI(Tl) is thus increased, leading to better energy resolution. Physical performance of the SPEM is adequate for clinical imaging, as shown by the reported results. The small size of the detector head allows the use of mechanical breast compression to minimize detection distance and tissue scatter (Fig. 1A). The market cost of the SPEM may be kept under one third of a conventional Anger camera, which allows the diffusion of the technique outside large teaching hospitals.

In the preliminary clinical test on 29 patients, the SPEM performed at least as well as a state-of-the-art conventional Anger camera. One more very small carcinoma was imaged (Figs. 4A and C) and all negative SPEM scans were equally negative by Anger camera. Moreover, the superior resolution of SPEM allowed a

more precise delineation of the cancer in patient 28 (Figs. 4B and D). This latter feature holds the promise of adding morphometric evaluation to ^{99m}Tc -MIBI uptake, which may prove useful for differential diagnosis of positive cases, such as malignant lesions versus benign positive lesions.

CONCLUSION

The SPEM prototype presented in this study allows high-resolution ^{99m}Tc -MIBI scintimammography in a clinical setting at a fraction of the cost of conventional Anger cameras or of solid-state prototype nuclear mammographs. Areas of improvement include better energy resolution and increased FOV.

ACKNOWLEDGMENTS

We thank Drs. M. Balan, K. Blazek and P. Maly at Preciosa Crytur, Turnov, Czech Republic, for assistance in SPEM development and setup. This work has been supported in part by a grant from Instituto Nazionale Fisica Nucleare-Consiglio Nazionale Ricerche-Ministero Dell'Universita e Della Ricerca Scientific e Tenologica.

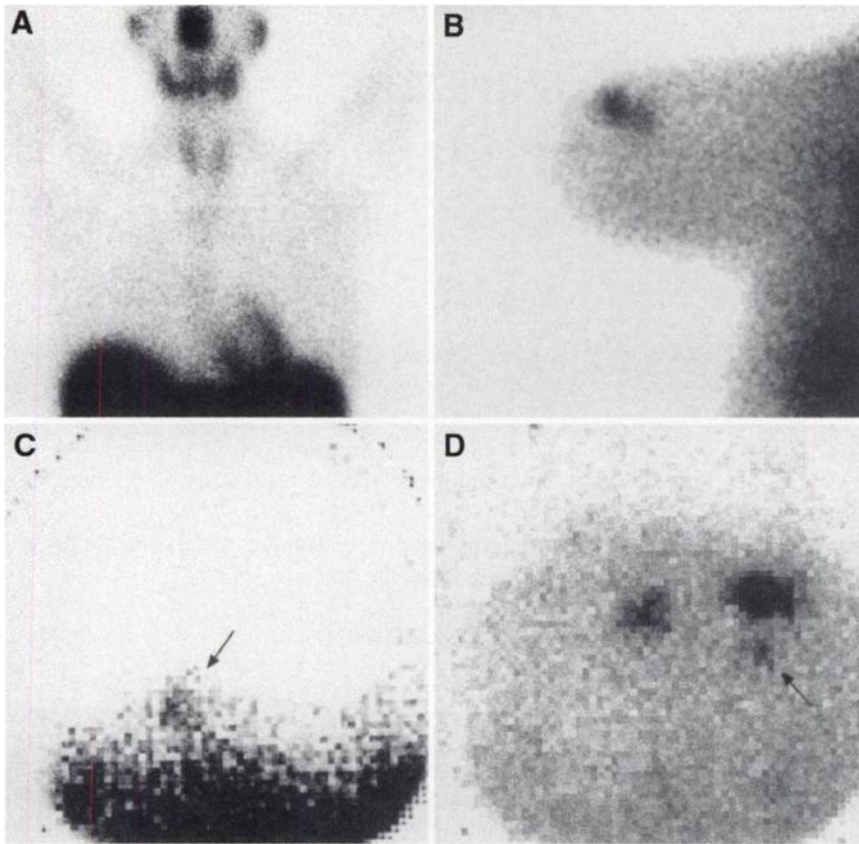


FIGURE 4. (A) Anger camera anterior view and (C) SPEM craniocaudal view of right breast in patient 1: small ductal carcinoma of 0.4 cm missed by Anger camera is well detected by SPEM. (B) Anger camera lateral view and (D) SPEM lateral view of left breast in patient 28: SPEM resolves as three separate lesions the irregular focal uptake seen in Anger camera scintimammograph.

REFERENCES

1. Khalkhali I, Mena I, Diggles L. Review of imaging techniques for the diagnosis of breast cancer: a new role of prone scintimammography using technetium-99m sestamibi. *Eur J Nucl Med.* 1994;21:357-362.
2. Kao CH, Wang SJ, Yeh SH. Technetium-99m MIBI uptake in breast carcinoma and axillary lymph node metastases. *Clin Nucl Med.* 1994;19:989-900.
3. Burak Z, Argon M, Mamix A, et al. Evaluation of palpable breast masses with Tc-99m MIBI: a comparative study with mammography and ultrasonography. *Nucl Med Commun.* 1994;15:604-612.
4. Taillefer R, Robidoux A, Lambert R, et al. Technetium-99m sestamibi prone scintimammography to detect primary breast cancer and axillary lymph node involvement. *J Nucl Med.* 1995;36:1758-1765.
5. Palmedo H, Schomburg A, Grunwald F, et al. Technetium-99m-MIBI scintimammography for suspicious breast lesions. *J Nucl Med.* 1996;37:626-630.
6. Khalkhali I, Villanave-Mayer J, Edell SL, et al. Diagnostic accuracy of ^{99m}Tc sestamibi breast imaging in the detection of breast cancer [abstract]. *J Nucl Med.* 1996;37:288P.
7. Palmedo H, Biersack S, Lastoria S, et al. Scintimammography with Tc-99m MIBI for breast cancer detection: results of the prospective European multicentric trial [abstract]. *J Nucl Med.* 1997;38:67P.
8. Maini CL, Tofani A, Sciuto R, et al. Technetium-99m-MIBI scintigraphy in the assessment of neoadjuvant chemotherapy in breast carcinoma. *J Nucl Med.* 1997;38:1546-1551.
9. Waxman AD. The role of Tc-99m-methoxyisobutylisonitrile in imaging breast cancer. *Semin Nucl Med.* 1997;27:40-54.
10. Buscombe JR, Cwikla JB, Thakrar DS, Hilson AJW. Scintigraphic imaging of breast cancer: a review. *Nucl Med Commun.* 1997;18:698-709.
11. Piwnica-Worms D, Chiu ML, Budding M, et al. Functional imaging of the multidrug-resistant P-glycoprotein with an organotechnetium complex. *Cancer Res.* 1993;53:977-984.
12. Ballinger JR, Hua HA, Berry BW, Firby P, Boxen I. ^{99m}Tc sestamibi as an agent for imaging P-glycoprotein-mediated multi-drug resistance: in vitro and in vivo studies in rat breast tumour cell lines and its doxorubicin-resistant variant. *Nucl Med Commun.* 1995;16:253-257.
13. Del Vecchio S, Ciarmiello A, Potena MI, et al. In vivo detection of multidrug resistant (MDR1) phenotype by technetium-99m sestamibi scan in untreated breast cancer. *Eur J Nucl Med.* 1997;24:150-159.
14. Duran-Cordobes M, Moretti JL, de Beco J, et al. Sestamibi Tc 99m uptake in human cell lines exhibiting MDR multidrug resistance. *Q J Nucl Med.* 1997;41:9.
15. Pani R, Pellegrini R, De Vincentis G, et al. SPEM: a dedicated camera for scintimammography. *Q J Nucl Med.* 1996;40:12.
16. Pani R, Pellegrini R, De Vincentis G, et al. Single photon emission mammography (SPEM): a new scintigraphic technique [abstract]. *Eur J Nucl Med.* 1995;22:876.
17. de Notaristefani F, Iacopi F, Malatesta T, Vittori F. High resolution small gamma cameras for SPET applications [abstract]. In: *Proceedings of SCINT'97 International Conference on Inorganic Scintillators, Shanghai, China;* 1997:12.
18. Blazek K, de Notaristefani F, Maly P, et al. YAP multicrystal gamma camera prototype. *IEEE Trans Nucl Sci.* 1995;42:1474-1482.
19. Pani R, Soluri A, Scopinaro F, et al. The role of Compton scattering in scintimammography. In: *Conference Record of the IEEE Nuclear Science Symposium and Medical Imaging Conference.* Anaheim, CA; 1996.
20. Palmedo H, Grunwald F, Bender H, et al. Scintimammography with technetium-99m methoxyisobutylisonitrile: comparison with mammography and magnetic resonance imaging. *Eur J Nucl Med.* 1996;23:940-946.
21. Tiling R, Khalkhali I, Sommer H, et al. Role of technetium-99m sestamibi scintimammography and contrast-enhanced magnetic resonance imaging for the evaluation of indeterminate mammograms. *Eur J Nucl Med.* 1997;24:1221-1229.
22. Patt BE, Ivanczyk JS, Tornai MP, Hoffmann EJ. Dedicated breast imaging system based on a novel solid state detector array [abstract]. *J Nucl Med.* 1997;38:142P.
23. Seidel J, Siegel S, Gandler WR, Green MV. Accuracy of event positioning in a pixellated BOG array coupled to a miniature position-sensitive phototube [abstract]. *J Nucl Med.* 1997;38:197P.
24. Pani R, Pellegrini R, Scopinaro F, et al. Portable gamma camera for clinical use in nuclear medicine. In: *Conference Record of the IEEE Nuclear Science Symposium and Medical Imaging Conference.* Anaheim, CA; 1996:1170-1174.
25. Pani R, Pellegrini R, Scopinaro F, et al. Scintillating array gamma camera for clinical use. *Nucl Industr Meth Phys Res.* 1997;392:295-298.
26. Becherer A, Helbich H, Staudenherz A, et al. The diagnostic value of planar and SPET scintimammography in different age group. *Nucl Med Commun.* 1997;18:710-718.
27. de Notaristefani F, Iacopi F, Malatesta T, Vittori F. Intrinsic performance of YAP:Ce and CsI: Tl needles for accurate medical imaging detectors [abstract]. In: *Proceedings of SCINT'97 International Conference on Inorganic Scintillators, Shanghai, China;* 1997:88.